THE JOURNAL OF PHYSICAL CHEMISTRY A

ARTICLE

pubs.acs.org/JPCA

Hydrolysis of a Chlorambucil Analogue. A DFT study.

F. P. Pineda,[‡] J. Ortega-Castro,[†,⊥] J. R. Alvarez-Idaboy,[§,⊥] J. Frau,[†,⊥] B. M. Cabrera,[‡] J. C. Ramírez,[‡] J. Donoso,[†,⊥] and F. Muñoz*[,†,⊥]

[†]Institut d'Investigació en Ciències de la Salut (IUNICS), Department de Química, Universitat de les Illes Balears, 07122 Palma de Mallorca, Spain

[‡]Facultad de Ciencias Químicas, Benemérita Universidad Autónoma de Puebla, Edificio 179, 18 Sur y Av. San Claudio, Col. San Manuel, 72570 Puebla, Puebla, México

[§]Facultad de Química, Departamento de Física y Química Teórica, Universidad Nacional Autónoma de México, México D.F. 04510, México

[⊥]Mexico-EU international collaboration network RMAYS, Universidad Nacional Autónoma de México, México D.F. 04510, México

Supporting Information

ABSTRACT: We study by density functional theory the hydrolysis of a chlorambucil analogue. Three SN_1 and one SN_2 mechanisms have been compared. Results show that the most likely mechanism involves the formation of an aziridinium ion via a first-order reaction subject to an energy barrier of 24.8 kcal/mol. Additionally, a kinetic study, using the thermodynamic formulation of the Transition State Theory, has been carried out. Theoretical results coincide with experimental values obtained under similar conditions of pH, temperature and chloride concentration.

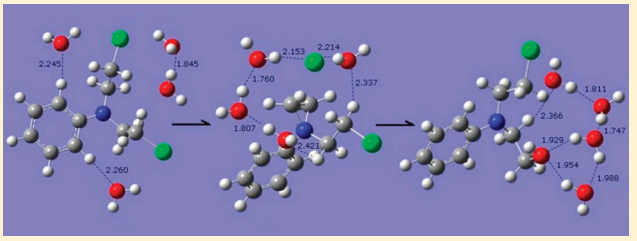

INTRODUCTION

The aromatic nitrogen mustard chlorambucil (**CLB**) has been extensively studied ever since it started to be used as an antitumor chemotherapeutic agent in the 1940s. Chlorambucil and melphalan are mainly used in the treatment of chronic lymphocytic leukemia,[1] but they are also indicated for Hodgkin's lymphoma, non-Hodgkin's lymphoma,[1,2] ovarian and breast cancer,[3] various other tumors, and certain autoimmune diseases.[4] The cytotoxicity of these compounds is due to their functions as alkylating agents, by means of the reaction with nucleophiles into the cell.[5] In fact, chlorambucil has been shown to bond covalently to DNA, RNA, and protein molecules in cells. Covalent bonding of these aryl nitrogen mustards to a DNA molecule can result in misreading of DNA code, DNA cross-linking, and, if cells are unable to repair the damage, to chain scissions[6] and subsequent cell death.[7] Usually, monofunctional and bifunctional alkylating compounds bond to DNA via nitrogen 7 in guanines. Aryl nitrogen mustards are scarcely selective and react with virtually all types of guanines.[8] However, N1 and N3 in adenine, N3 in cytosine, and O6 in guanine, as well as phosphate groups in DNA strands and proteins, provide additional potential sites for bonding of these compounds. In bifunctional compounds such as the nitrogen mustard, the second side chain 2-chloroethyl can alkylate a second guanine molecule, thereby establishing cross-linkages which can seriously disturb nucleic acid function. Such linkages were recently studied by examining the adducts between CLB and DNA.[9,10]

The hydrolysis of aliphatic and aromatic nitrogen mustards has been extensively studied. The most widely accepted mechanism[11,12] for this reaction involves the formation of an aziridinium ion intermediate (**2** in Scheme 1), followed by an external nucleophilic attack. Some authors, however, favor a SN_1 instead of a SN_2 mechanism.[13−20] Also, reactions with powerful nucleophiles can proceed via inter- and intramolecular pathways as well.[5] Gamcsik et al.[21] failed to directly detect the aziridinium intermediates of melphalan and chlorambucil in solution by ^{1}H NMR. Various factors including nucleophile strength,[5] the protonation state of the amine (pH),[22] temperature and the common ion effect have been examined as potential sources of variability in the reaction pathway and hence in the hydrolysis mechanism for nitrogen mustards.[23]

A number of kinetic studies on a variety of aromatic nitrogen mustards have been reported. Thus, O'Connor et al.[22] studied the hydrolysis kinetics of the $Ar-X-C_6H_4-N(CH_2CH_2Cl)_2$ series, with X = O, CH_2, CONH, S, CO, and SO_2, and used an iterative curve-fitting procedure to determine the first-order rate constant for the first (k_1) and second (k_2) steps. Cullis et al.[23] obtained the rate constants of chlorambucil and the chlorambucil−spermidine conjugate at 37 °C over the pH range 1.5−8.0 and examined the variation of k_{obs} via the chloride ion

Received: November 24, 2010
Revised: February 3, 2011
Published: March 01, 2011

Scheme 1. Mechanisms Proposed of Hydrolysis of *N,N*-Bis(2-chloroethyl)benzenamine

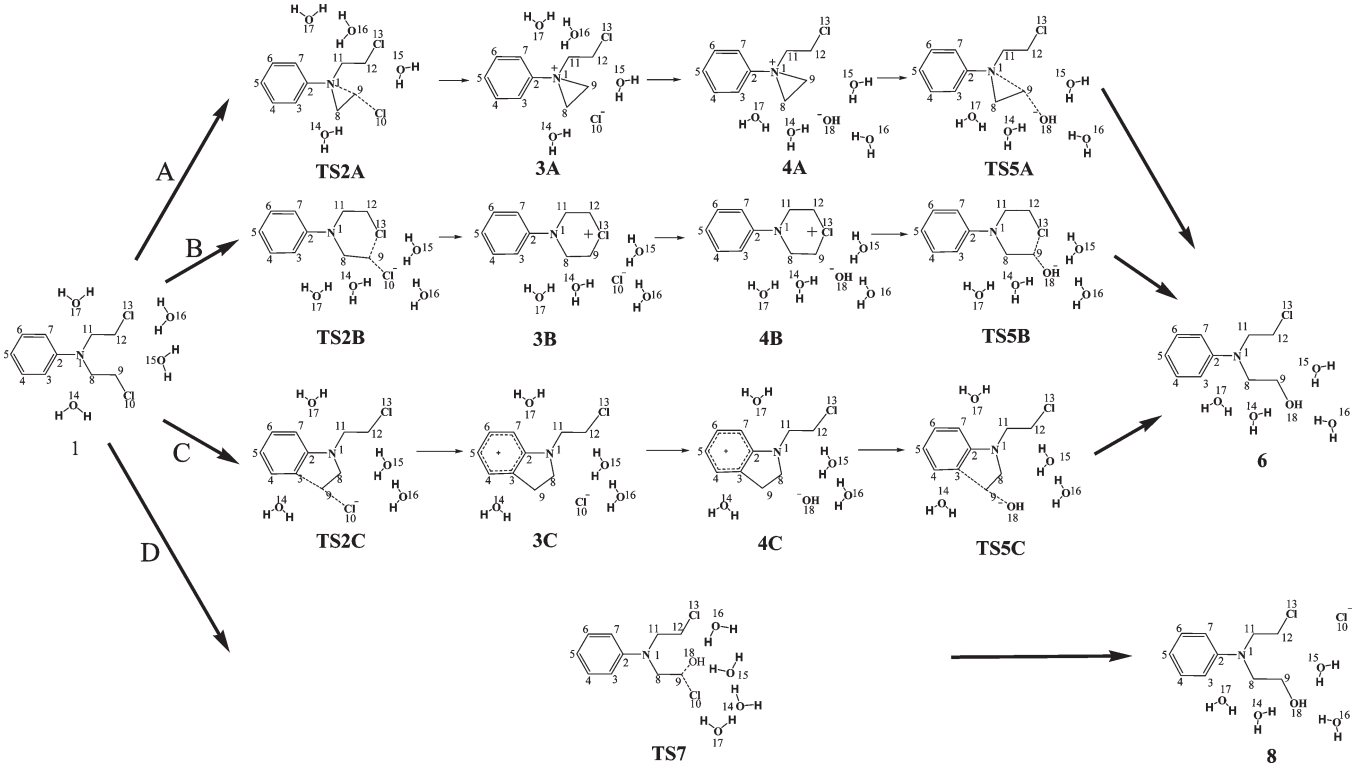

concentration in phosphate buffer at pH 7. Pettersson−Fernholm et al.[4] studied the hydrolysis of 4-bis(2-chloroethyl)aminophenylacetic acid (PAM) in an aqueous medium and proposed a first-order mechanism for the entire pH range examined. These authors also investigated the reactions of the biological nucleophiles glutathione (GSH) and thiocyanate ion with PAM. Similar studies have also been conducted on chloroacetanilide herbicides in aqueous solutions.[12]

In this work, we used DFT methodology to study the hydrolysis of the **CLB** analogue *N,N-bis*(2-chloroethyl)benzenamine (**1** in Scheme 1). Four potential pathways were examined, namely: three intramolecular SN_1 mechanisms (A, B, and C in Scheme 1); and an intermolecular SN_2 mechanism (D in Scheme 1). A kinetic study of the most likely mechanism was also conducted and the results compared with available experimental data.

METHODOLOGY

Computational details. The target compound was the chlorambucil analogue *N,N*-bis(2-chloroethyl) benzenamine (**1**). It has been chosen for the study of the hydrolysis of aromatic nitrogen mustard. Cullis et al.[23] obtained a similar kinetic constant (k_{obs}) for chlorambucil (benzenebutanoic acid, 4-[bis-(2-chloroethyl)amino]-) and the chlorambucil−spermidine conjugate (benzenebutanamide, *N*-[3-[(4-aminobutyl)(3-aminopropyl)-amino]propyl]-4-[bis(2-chloroethyl)amino]-), which suggests that the reaction rate of the nitrogen mustard is unaffected by polyamine conjugation. For this reason, the removal of butyric acid of the CLB structure should not affect the hydrolysis mechanisms proposed in this work.

DFT calculations were performed with the Gaussian09 software package.[24] All structures (reactants, products, intermediates and transition states) were fully optimized at the M06-2X level,[25,26] using the 6-31+G(d,p) basis set in combination with the Cosmo polarizable continuum method (CPCM)[27,28] in order to mimic the water solvent effect. Additionally four explicit water molecules were added to all structures.

The M06-2X functional is a new hybrid meta exchange correlation functional proposed recently by Zhao and Truhlar, and has been recommended for applications involving kinetics and noncovalent interactions.[25,26] CPCM is an implementation of the Cosmo model in the framework of the polarizable continuum model (PCM) formalism and is one of the most used and reliable continuum salvation procedures.[28−30]

The structures thus obtained were subjected to vibrational analysis calculations toward their characterization as local minima (all positive force constants) or transition states (one imaginary force constant only). The standard state was taken to be 1 atm, which is the default choice in Gaussian calculations.

The kinetic values obtained for the most likely mechanisms were reoptimized with the SMD (solvation model density) continuum method in order to improve fitting. SMD is a universal solvation model based on the polarized continuous quantum mechanical charge density of the solute. This method achieves accurate values of solvation free energies.[31]

Kinetic Calculations. Calculated ΔG values were subjected to various thermodynamic corrections in order to facilitate comparison with experimental data. Thus, the standard state for ΔG values was changed from 1 atm to 1 M in order to relate the calculated Gibbs free-energies of activation with experimental

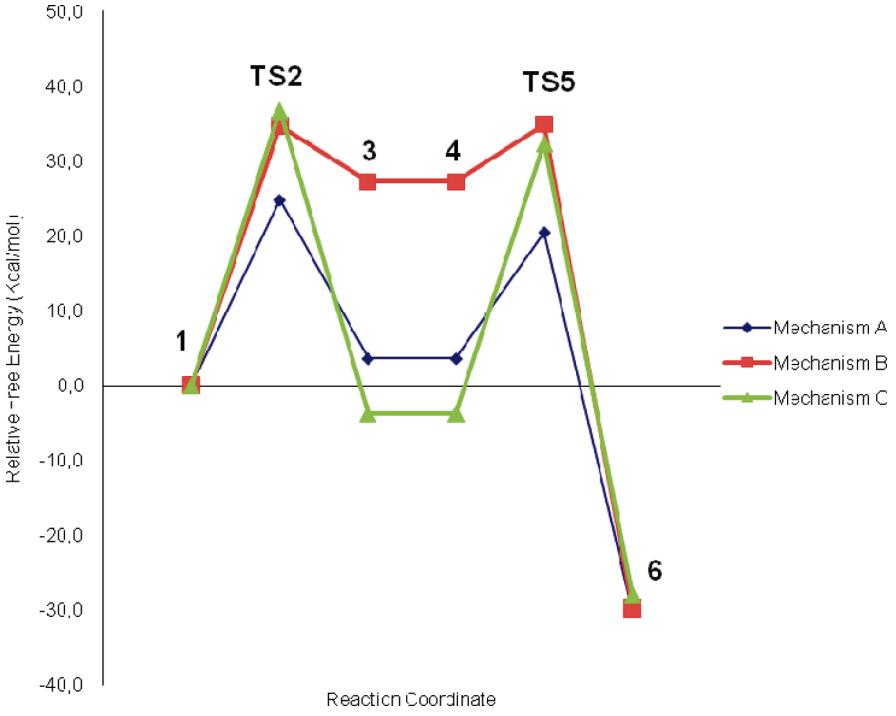

Figure 1. Energy profiles for the reactions of hydrolysis with *N*,*N*-bis(2-chloroethyl)benzenamine in solvated phase (CPCM) with M06-2X/6-31+G(d,p) method.

Table 1. Main Geometric Data[a] for the Structures Involved in the Reaction of Hydrolysis of *N*,*N*-Bis(2-chloroethyl)benzenamine

		mechanism A				mechanism B				mechanism C				mechanism D	
	1	**TS2A**	**3A**	**4A**	**TS5A**	**TS2B**	**3B**	**4B**	**TS5B**	**TS2C**	**3C**	**4C**	**TS5C**	**SN_2**	**6/8**
N1−C8	1.451	1.471	1.486	1.501	1.482	1.450	1.457	1.458	1.451	1.460	1.481	1.482	1.460	1.449	1.459/1.467
N1−C11	1.450	1.470	1.501	1.490	1.470	1.451	1.463	1.467	1.451	1.452	1.460	1.457	1.450	1.451	1.459/1.473
N1−C2	1.392	1.429	1.465	1.472	1.441	1.404	1.425	1.424	1.406	1.362	1.302	1.304	1.348	1.390	1.402/1.432
N1−C9	2.467	1.902	1.488	1.501	1.797										
C8−C9	1.527	1.463	1.479	1.469	1.457	1.505	1.509	1.511	1.508	1.531	1.532	1.530	1.532	1.541	1.525/1.540
C9−C3	3.337									2.154	1.540	1.540	2.045		
C9−Cl10	1.813	2.349	4.583			2.612	3.613			2.421	3.656			2.255	-
C9−O18	-			3.275	2.094			4.346	2.345			3.132	2.095	2.100	1.429/1.469
C11−C12	1.527	1.525	1.519	1.522	1.523	1.520	1.508	1.509	1.520	1.526	1.525	1.526	1.526	1.524	1.522/1.522
C12−Cl13	1.810	1.801	1.798	1.793	1.795	1.822	1.844	1.845	1.830	1.804	1.800	1.796	1.802	1.808	1.806/1.800
C9−Cl13						2.328	1.844	1.841	2.199						
N1−C8−C9	111.8	80.8	60.3	60.7	83.5	114.5	111.7	111.3	114.1	107.7	102.5	102.1	107.2	118.9	111.3/108.3
C8−C9−Cl10	109.7	106.4	45.5			100.5	109.7			96.3	73.4			94.0	-
C8−C9−O18	-			84.5	105.6			100.7	95.0			73.1	90.4	104.8	110.5/106.1
C8−C9−C3										85.9	101.5	100.9	88.6		
C11−N1−C2−C3	179.5	173.0	98.5	173.8	168.8	157.3	117.8	117.4	164.0	171.3	174.8	179.6	177.6	178.8	144.2/165.2

[a] Distances in Å and angles in deg.

rate coefficients, which are reported in concentration units. Changing the standard state reduced ΔG values at 298.15 K by 1.89 kcal/mol for bimolecular reactions. We also used the approach of Benson[32] based on which ΔG is 2.56 kcal/mol lower in solution at 298.15 K than in the gas phase (ΔG_{gas}) in bimolecular reactions. A more detailed description of these corrections can be found elsewhere.[33] These corrections were used recently for the kinetic of Baeyer Villinger reaction with excellent agreement with experimental result.[34]

Individual rate constants were calculated by using the thermodynamic formulation of the transition state theory (TST):[35−37]

$$k_i = \sigma\kappa\frac{k_B T}{h}\exp\left(\frac{-\Delta G^{\ddagger}}{RT}\right) \quad (1)$$

where κ is the tunnelling correction, σ the reaction path degeneracy, $\Delta G^{\ddagger}$ the Gibbs free energy of activation at temperature T, and k_B and h are the Boltzmann and Planck constants,

Table 2. ΔG (kcal/mol) at 298.15 K for the Structures Involved in the Reaction Computed at the Level of Theory: M06-2X/6-31+G(d,p) with CPCM/SMD Approach

structure	mechanism A [OH^-] CPCM/SMD	mechanism A [H_2O] SMD	mechanism B [OH^-] CPCM	mechanism C [OH^-] CPCM	structure	mechanism D [OH^-] CPCM
1	0.0/0.0	0.0	0.0	0.0	**1**	0.0
TS2	24.8/24.2	24.2	34.7	36.8		
3	3.6/2.8	2.8	27.2	−3.7		
					TS7	27.0
4	3.6/2.8	2.8	27.2	−3.7		
TS5	20.5/21.6	28.5	34.9	32.4		
6	−30.3/−31.8	−31.8	−29.8	−28.0	**8**	−19.7

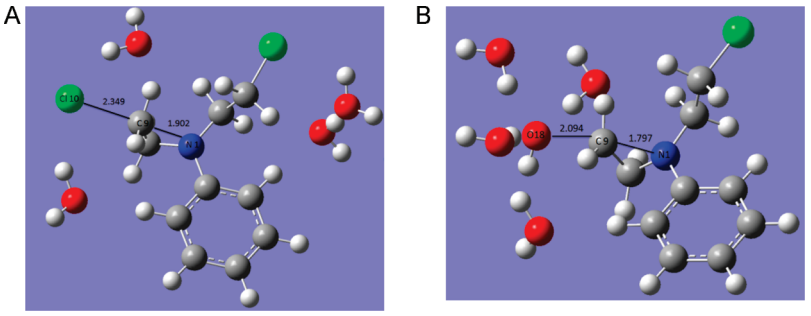

Figure 2. (A) Transition state of the formation of the aziridinium intermediate, **TS2A** (interatomic distances in Å). (B) Transition state of the cleavage of the aziridinium intermediate, **TS2B** (interatomic distances in Å).

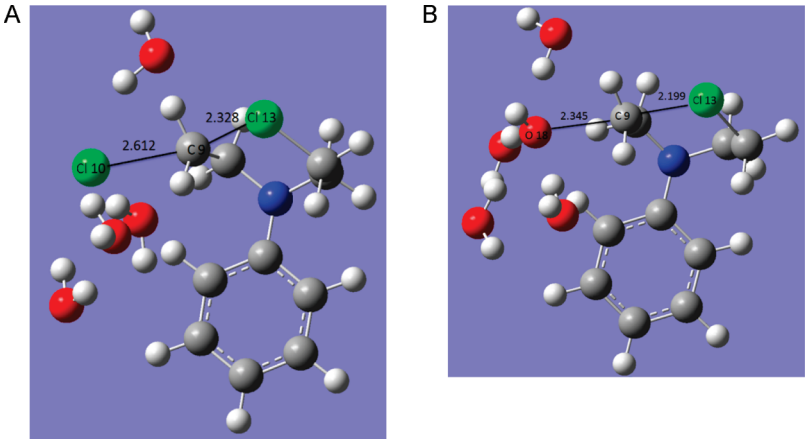

Figure 3. (A) Transition state of the formation of the six members intermediate, **TS3A** (interatomic distances in Å). (B) Transition state of the cleavage of the aziridinium intermediate, **TS3B** (interatomic distances in Å).

respectively. A unity tunnelling correction was used since transition states involved heavy atoms motions.[38]

RESULTS AND DISCUSSION

The hydrolysis mechanism of *N*,*N*-bis(2-chloroethyl)-benzenamine (**1**) was examined in the light of four different pathways (Scheme 1). Pathways A, B and C involved two separate stages, namely: (1) formation of a carbocation (**3A**, **3B**, and **3C**, respectively); (2) hydrolysis of the carbocation and formation of 2[(*N*-(2-chloroethyl)-*N*-phenylamino]ethanol (**6**). On the other hand, mechanism D involved no intermediate, since it is a SN_2 mechanism. Figure 1 shows the energy profiles in the solvated phase for pathways A, B, and C. Table 1 lists the most salient geometric parameters for the four mechanisms and Table 2 the relative free energies, ΔG, of the structures involved in the process. Pictures of all structures of Scheme 1 can be found in the Supporting Information.

Mechanism A. This mechanism started with the concerted relase of Cl10 and formation of an aziridinium cycle via an intramolecular nucleophilic attack (see Scheme 1). The transition state for this process (**TS2A**) occurred at an N1−C9 distance of 1.902 Å and a C9−Cl10 distance of 2.349 Å (Figure 2A). The energy barrier for the first step was 24.8 kcal/mol (Table 2, Figure 1). The aziridinium intermediate (**3A**) was 3.6 kcal/mol more unstable than the starting compound (**1**), which is consistent with the experimental results of tests where no intermediate was detected.[21]

The process was continued by replacing the Cl^- ion with a hydroxyl group and equaling the energy of the two states. This

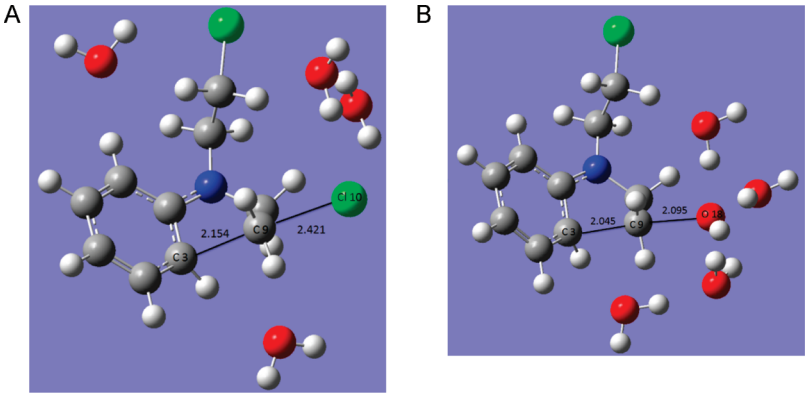

Figure 4. (A) Transition state of the formation of the indole intermediate, **TS4A** (interatomic distances in Å). (B) Transition state of the cleavage of the aziridinium intermediate, **TS4B** (interatomic distances in Å).

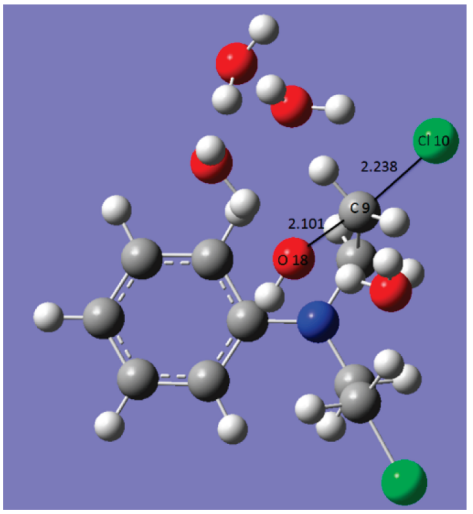

Figure 5. Transition state of the SN_2 mechanism, **TS7** (interatomic distances in Å).

avoided a potential interference of the Cl atom with the attack on the hydroxyl group. Therefore, the starting structure for the second half-reaction was structure **4A**. The hydroxyl group was placed at a distance of 3.275 Å from C9 and an angle of attack (O18−C9−C8) of 84.5°. Raising the energy profile led to transition state **TS5A**, where a nucleophilic attack of the hydroxyl group occurred in a concerted manner with cleavage of the aziridinium intermediate (Figure 2B). The energy barrier for the second step was 16.9 kcal/mol.

Mechanism B. The second mechanism started with a concerted process involving release of the Cl10 atom and formation of a six-member intermediate. The corresponding transition state (**TS2B** in Scheme 1, Figure 3A) exhibited four water molecules around the Cl atom, the average distance from which, 2.35 Å, facilitated its release. The energy barrier for this first half-reaction was 34.7 kcal/mol and thus higher than in mechanism A. Downhill from this transition state structure, the system evolved to the adduct **3B**, which was 27.2 kcal/mol more unstable than the starting reactant (**1**).

Chlorine atom was replaced with a hydroxyl group placed at 4.346 Å and an angle of attack (C8−C9−O18) of 100.7° with respect to C9 (**4B**). The second step of this mechanism involved concerted opening of the cycle and nucleophilic attack, occurred via **TS5B**, which was subject to an energy barrier of only 7.7 kcal/mol (Figure 3B). The final product (**6**) was more stable than its preceding structure.

Mechanism C. Like the previous two mechanisms, C started with a concerted process: release of the Cl atom and formation of a five-member indoline ring (TS2C in Figure 4A). As can be seen from Table 1, the C9−C3 distance decreased from 3.337 to 1.540 Å during the half-reaction and led to an intermediate 3.7 kcal/mol more stable than the starting reactant (1). The process was continued with the concerted opening of the imidazole ring and nucleophilic attack of the hydroxyl group (Table 1, Figure 4B).

Mechanism C was the most thermodynamically unfavorable as it exhibited the highest energy barriers: 36.8 kcal/mol for the first half-reaction and 36.1 kcal/mol for the second.

Mechanism D. Unlike the previous three mechanisms, D involved the simultaneous, concerted attack of the hydroxyl group and release of the Cl atom in **1** (Figure 5), so it was a bimolecular substitution (SN_2) mechanism. The final reaction product is the compound **6** plus a Cl^- ion (**8** in Scheme 1). The energy barrier was 2.2 kcal/mol higher than that for the rate-determining step in mechanism A.

A comparison of the three intramolecular mechanisms (A, B, and C) based on their ΔG values (Figure 1) revealed that the most likely among them was that involving the formation of an aziridinium ion via a first-order reaction subject to an energy barrier of 24.8 kcal/mol. The low stability of the aziridinium intermediate is consistent with experimental results.[21] On the other hand, ΔG for mechanism D (SN_2) was 27.0 kcal/mol, which is only 2.2 kcal/mol higher than the value for the aziridinium mechanism. In the past it was thought that the only possible mechanism would be of SN_2 type. Benn et al.[5] suggested that the mechanism may proceed by either of two competitive processes: one involving direct displacement (SN_2), and the other proceeding by way of aziridinium ion reactive intermediate. The aziridinium ion pathway seems to be preferred, except in reactions involving very powerful nucleophiles. Gamcsik et al.[21] used ^1H NMR spectroscopy to confirm the mechanism involving the aziridinium intermediate for melphalan and chlorambucil, but failed to detect it in solution. Other derivatives such as chloroacetanilide herbicides were studied in the light of an SN_2 mechanism and found to exhibit an anomalously high reactivity potentially resulting from the presence of an aziridinium intermediate somewhere in the process.[12]

The similarity between the energy barriers for mechanisms A and D suggests that they might be two competitive processes.

Scheme 2. Mechanism of Formation of the 2-(*N*-(2-chloroethyl)-*N*-phenylamino)ethanol (6) via SN_1, Where R−Cl = 1, R^+ = TS2A, and R−OH = 6[a]

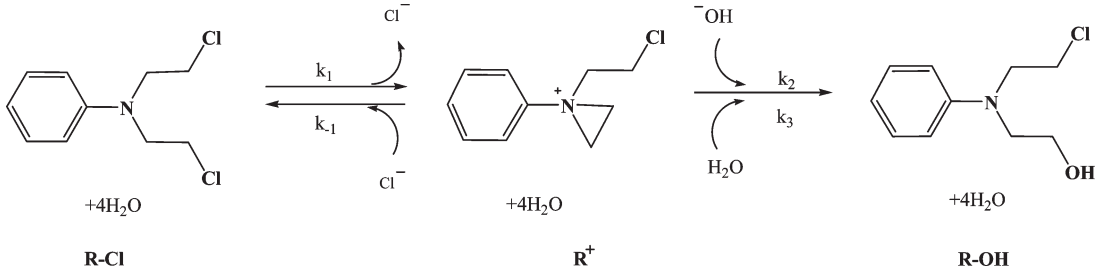

[a] k_1 and k_{-1} are the direct and reverse aziridinium intermediate formation kinetic constants, k_2 is the formation kinetic constant of **6** when the nucleophile is hydroxyl ion, and k_3 is the formation kinetic constant of **6** when the nucleophile is water.

Table 3. Kinetic Constants for the Reactions of Hydrolysis of *N,N*-Bis(2-chloroethyl)benzenamine Exposed in Scheme [2] (pH =7.35, $[Cl^-]$ = 0.1 M, $[OH^-]$ = 2.24 × 10^{-7} M, $[H_2O]$ = 55.5 M)[a]

T (K)	k_1 (s^{-1})	k_{-1} (s^{-1} M^{-1})	k_2 (s^{-1} M^{-1})	k_3 (s^{-1} M^{-1})	k_{-1} [Cl]	k_2 [OH^-]	k_3 [H_2O]	k_{ef} (s^{-1})
298	1.50×10^{-4}	1.27×10^{-3}	1.03×10^{-1}	8.45×10^{-7}	1.27×10^{-4}	2.31×10^{-8}	4.74×10^{-5}	4.10×10^{-5}
300	2.01×10^{-4}	1.47×10^{-3}	1.21×10^{-1}	9.96×10^{-7}	1.47×10^{-4}	2.71×10^{-8}	5.53×10^{-5}	5.50×10^{-5}
302	2.67×10^{-4}	1.70×10^{-3}	1.42×10^{-1}	1.16×10^{-6}	1.70×10^{-4}	3.18×10^{-8}	6.44×10^{-5}	7.34×10^{-5}
304	3.53×10^{-4}	1.96×10^{-3}	1.66×10^{-1}	1.35×10^{-6}	1.96×10^{-4}	3.72×10^{-8}	7.49×10^{-5}	9.77×10^{-5}
306	4.66×10^{-4}	2.26×10^{-3}	1.94×10^{-1}	1.57×10^{-6}	2.26×10^{-4}	4.34×10^{-8}	8.69×10^{-5}	1.29×10^{-4}
308	6.13×10^{-4}	2.60×10^{-3}	2.26×10^{-1}	1.82×10^{-6}	2.60×10^{-4}	5.06×10^{-8}	1.01×10^{-4}	1.71×10^{-4}
310	8.03×10^{-4}	2.99×10^{-3}	2.63×10^{-1}	2.09×10^{-6}	2.99×10^{-4}	5.88×10^{-8}	1.16×10^{-4}	2.25×10^{-4}

[a] Experimental data: CLB (k_{ef} = 6.12 × 10^{-4} s^{-1}; pH = 7, 310 K),[23] S-CLB (k_{ef} = 5.52 × 10^{-4} s^{-1}; pH = 7, 310 K),[23] PAM (k_{ef} = 3.15 × 10^{-4} s^{-1}, pH = 7.5, $[Cl^-]$ = 0.11M, 310 K),[4] and (k_{ef} = 3.84 × 10^{-4} s^{-1}, pH = 7.0, $[Cl^-]$ = 0.10M, 310 K).[4]

Table 4. First Order Rate Constant for the Hydrolysis of CEB at 310 K at Different pH

pH	k (s^{-1})	log k_{ef}
3	1.19×10^{-4}	−3.92
4	1.19×10^{-4}	−3.92
5	1.19×10^{-4}	−3.92
6	1.19×10^{-4}	−3.92
7	1.19×10^{-4}	−3.92
8	1.19×10^{-4}	−3.92
9	1.22×10^{-4}	−3.91
10	1.46×10^{-4}	−3.84
11	3.89×10^{-4}	−3.41
12	2.81×10^{-3}	−2.55
13	2.71×10^{-2}	−1.57
14	2.70×10^{-1}	−0.57

Their reaction rates should be affected by the reactant concentrations. Whereas the rate of A, a first-order mechanism, was only affected by the concentration of **1**, mechanism D was second-order in **1** and hydroxyl ion. Because the $[OH^-]$ concentration was ca. 10^{-7}, the mechanism involving the formation of an aziridinium ion was more favorable, even though the energy barriers were similar.

Kinetic Calculations. Scheme 2 shows the most likely kinetic mechanism for 2-[*N*-(2-chloroethyl)-*N*-phenylamino]ethanol (mechanism A in Scheme 1), which involves two steps, namely: (1) formation of the unstable aziridinium intermediate in equilibrium with the CLB analogue **1**, which is slow; and (2) formation of the end product (**6**), which is faster.

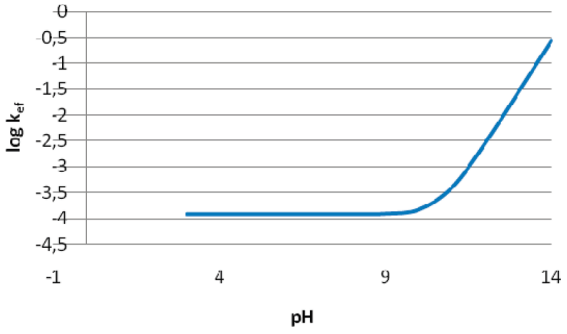

Figure 6. pH-rate profile for of hydrolysis of **1** based on the data summarized in Table 4.

In this work, we conducted a kinetic study the hydrolysis of **1** (R−Cl in the kinetic equation) and compared the results with reported experimental values (Table 3). Table 2 (columns 2 and 3) shows the reoptimized Gibbs free energy values using SMD continuum method for both nucleophiles involved in this kinetic study: OH^- and H_2O. The study of the chlorambucil analogue was facilitated by the fact that the different groups in *para* to aniline had little effect on the reaction rate. This is reflected in the kinetic constants of chlorambucil (6.12 × 10^{-4} s^{-1} at pH 7 at 310 K) and the chlorambucil−spermidine conjugate (S−CLB, 5.52 × 10^{-4} s^{-1} at pH 7 at 310 K), which differed only in their *para* substituent.[23] UV spectroscopy measurements provided a

dx.doi.org/10.1021/jp111202p |*J. Phys. Chem. A* 2011, 115, 2359–2366

pK_a value of 2.3 and 2.0−2.3 for the ionizable arylamine group in CLB and S−CLB, respectively. This confirmed that the model used to study the hydrolysis of **1** at neutral pH was accurate. Some authors have performed kinetic studies of the hydrolysis of other CLB analogues such as 4-bis(2-chloroethyl)amino-phenylacetic acid (PAM),[4] the first-order kinetic constants were 3.15×10^{-4} s^{-1} (pH 7.5, 310 K, [Cl$^-$] = 0.11 M) and 3.84×10^{-4} s^{-1} (pH 7.0, 310 K, [Cl$^-$] = 0.10 M), respectively.

On the basis of the mechanism of Scheme 2, if the first half-reaction is reversible and assumed to be the rate-determining step, then the rate of disappearance of the CLB analogue will be given by

$$-\frac{d[R-Cl]}{dt} = k_1[R-Cl] - k_{-1}[R^+][Cl^-] \quad (2)$$

Applying the stationary state condition to the aziridinium intermediate gives

$$+\frac{d[R^+]}{dt} = k_1[R-Cl] - k_{-1}[R^+][Cl^-] - k_2[R^+][OH^-] - k_3[R^+][H_2O] = 0 \quad (3)$$

Rearrangement of which provides the aziridinium ion concentration:

$$[R^+] = \frac{k_1[R-Cl]}{k_{-1}[Cl^-] + k_2[OH^-] + k_3[H_2O]} \quad (4)$$

Substituting such a concentration into eq 2 yields

$$-\frac{d[R-Cl]}{dt} = \frac{k_1(k_2[OH^-] + k_3[H_2O])[R-Cl]}{k_{-1}[Cl^-] + k_2[OH^-] + k_3[H_2O]} \quad (5)$$

where

$$k_{ef} = \frac{k_1(k_2[OH^-] + k_3[H_2O])}{k_{-1}[Cl^-] + k_2[OH^-] + k_3[H_2O]} \quad (6)$$

Our kinetic study was based on the thermodynamic data for mechanism A in Table 2 and the SMD solvation model. Table 3 lists the results for the direct and reverse aziridinium intermediate formation kinetic constants (k_1 and k_{-1}), as well as the kinetic constants for the formation of the end product (k_2 and k_3) (Scheme 2). The kinetics of formation of the aziridinium ion was first-order. Table 3 also shows the values of kinetic constants multiplied by the nucleophile concentration.

As can be seen from Table 3, the kinetic constant k_2 was 5 orders of magnitude greater than k_3, which is consistent with the fact that hydroxyl ion is a very strong nucleophile relative to water; at pH 7, however, the concentration of water is 9 orders of magnitude higher than the typical concentration of hydroxyl ion in the environment. Therefore, at neutral pH water is the principal nucleophile in this reaction. The situation changed as the hydroxyl concentration was increased by raising the pH to alkaline values. On the basis of the foregoing, the general case (eq 6) was simplified by assuming water to be the only nucleophile acting in the hydrolysis process:

$$k_{ef} = \frac{k_1k_2[H_2O]}{k_{-1}[Cl^-] + k_2[H_2O]} \quad (7)$$

Above pH 7, the hydroxyl ion concentration becomes more influential and a double hydrolysis between this ion and water can take place, in which case the general eq 6 is applicable.

Table 4 shows a series of k_{ef} values obtained over the pH range 3−14 by using [Cl$^-$] = 0.1 M and [H_2O] = 55.5 M in eq 6. The results coincided with experimental values obtained under similar conditions as regards pH, temperature and chloride concentration. Consistent with the predictions, k_{ef} remained virtually constant from pH 4 to 8; also, it exhibited an exponential variation with the hydroxyl ion concentration above pH 9 (Figure 6).

It is important to highlight that theoretical calculations confirm that the most favorable mechanism of hydrolysis occurs through the formation of an aziridinium intermediate, discarding a SN_2 type reaction. Additionally kinetic theoretical results coincide with experimental values obtained under similar conditions of pH, temperature, and chloride concentration.

■ ASSOCIATED CONTENT

Supporting Information. Pictures of all structures presented in Scheme 1. This material is available free of charge via the Internet at http://pubs.acs.org.

■ ACKNOWLEDGMENT

This work was funded by the Spanish Government in the framework of Project CTQ2008-02207/BQU. The authors are grateful to Centro de Cálculo de Computación de Galicia (CESGA), and Centro de Cálculo de Computación de Cataluña (CESCA), for access to their computational facilities. This work is the result of the Mexico-EU international collaboration network RMAYS, funded by FONCICYT, Project No. 94666.

■ REFERENCES

(1) Faguet, C. B. *J. Clin. Oncol.* **1994**, *12*, 1974–1990.
(2) Wöhrer, S.; Raderer, M.; Kaufmann, H.; Hejna, M.; Chott, A.; Zelinski, C.; Drach, J. *Onkologie* **2005**, *28*, 73–78.
(3) McCully, K. S.; Narayansingh, G. V.; Cumming, G. P.; Sarkar, T. K.; Parkin, D. E. *Scot. Med. J.* **2000**, *45*, 51–53.
(4) Pettersson-Fernholm, T.; Vilpo, J.; Kosonen, M.; Hakala, K.; Hovinen, J. *J. Chem. Soc., Perkin Trans.* **1999**, *2*, 2183–2187.
(5) Benn, M. H.; Kazmaier, P.; Watanatada, C.; Owen, L. N. *Chem. Commun.* **1970**, 1685–1686.
(6) Singer, B.; Kusmierek, J. T. *Annu. Rev. Biochem.* **1982**, *52*, 655–693.
(7) Lind, M. J.; Ardiet, C. *Cancer Surveys* **1993**, *17*, 157–188.
(8) Brendel, M.; Ruhland, A. *Mutat. Res.* **1984**, *133*, 51–85.
(9) Mohamed, D.; Shereen, M.; Thomale, J.; Linscheid, M. W. *Chem. Res. Toxicol.* **2009**, *22*, 1435–1446.
(10) Florea-Wang, D.; Pawlowicz, A. J.; Sinkkonen, J.; Kronberg, L.; Vilpo, J.; Hovinen, J. *Chem. Biodiv.* **2009**, *6*, 1002–1013.
(11) Golding, B. T.; Kebbell, M. J.; Lockhart, J. M. *J. Chem. Soc., Perkin Trans.* **1987**, *2*, 705–713.
(12) Lippa, K. A.; Demel, S.; Lau, I. H.; Roberts, A. L. *J. Agric. Food Chem.* **2004**, *52*, 3010–3021.
(13) Bardos, T. J.; Datta-Gupta, N.; Hebborn, P.; Triggle, D. J. *J. Med. Chem.* **1965**, *8*, 167–174.
(14) Everett, J. L.; Roberts, J. J.; Ross, W. C. J. *J. Chem Soc.* **1953**, 2386–2392.
(15) Ross, S. D. *J. Am. Chem. Soc.* **1947**, *69*, 2982–2983.
(16) Ross, W. C. J. *Adv. Cancer Res.* **1953**, *1*, 397–449.
(17) Levins, P. L.; Papanastassiou, Z. B. *J. Am. Chem. Soc.* **1965**, *87*, 826–831.

(18) Rutman, R. J.; Chun, E. H. L.; Jones, J. *Biochem. Biophys. Acta* **1969**, *174*, 663–673.
(19) Price, C. C.; Gancher, G. M.; Koneru, P.; Shibakawa, R.; Sower, J. R.; Yamaguchi., M. *Ann. N.Y. Acad. Sci.* **1969**, *163*, 593–613.
(20) Chapman, N. B.; James, J. W. *J. Chem. Soc.* **1954**, 2103–2108.
(21) Gamcsik, M. P.; Millis, K. K.; Hamill, T. G. *Chem-Bio. Interac.* **1997**, *105*, 35–52.
(22) O'Connor, C. J.; Denny, W.; Fan, Y.-J.; Gravatt, G.; Grignor, B.; McLennan, D. *J. Chem. Soc., Perkin Trans 2* **1991**, 1933–1939.
(23) Cullis, P. M.; Green, R. E.; Malone, M. E. *J. Chem. Soc., Perkin Trans. 2* **1995**, 1503–1511.
(24) Gaussian 09, Revision A.1, Frisch, M. J.; Trucks, G. W.; Schlegel, H. B.; Scuseria, G. E.; Robb, M. A.; Cheeseman, J. R.; Scalmani, G.; Barone, V.; Mennucci, B.; Petersson, G. A.; Nakatsuji, H.; Caricato, M.; Li, X.; Hratchian, H. P.; Izmaylov, A. F.; Bloino, J.; Zheng, G.; Sonnenberg, J. L.; Hada, M.; Ehara, M.; Toyota, K.; Fukuda, R.; Hasegawa, J.; Ishida, M.; Nakajima, T.; Honda, Y.; Kitao, O.; Nakai, H.; Vreven, T.; Montgomery, J. A., Jr.; Peralta, J. E.; Ogliaro, F.; Bearpark, M.; Heyd, J. J.; Brothers, E.; Kudin, K. N.; Staroverov, V. N.; Kobayashi, R.; Normand, J.; Raghavachari, K.; Rendell, A.; Burant, J. C.; Iyengar, S. S.; Tomasi, J.; Cossi, M.; Rega, N.; Millam, N. J.; Klene, M.; Knox, J. E.; Cross, J. B.; Bakken, V.; Adamo, C.; Jaramillo, J.; Gomperts, R.; Stratmann, R. E.; Yazyev, O.; Austin, A. J.; Cammi, R.; Pomelli, C.; Ochterski, J. W.; Martin, R. L.; Morokuma, K.; Zakrzewski, V. G.; Voth, G. A.; Salvador, P.; Dannenberg, J. J.; Dapprich, S.; Daniels, A. D.; Farkas, Ö.; Foresman, J. B.; Ortiz, J. V.; Cioslowski, J.; Fox, D. J. Gaussian, Inc.: Wallingford CT, 2009.
(25) Zhao, Y.; Truhlar, D. G. *Theor. Chem. Acc.* **2008**, *120*, 215–227.
(26) Zhao, Y.; Truhlar, D. G. *Acc. Chem. Res.* **2008**, *41*, 157–167.
(27) Barone, V.; Cossi, M. J. *Phys. Chem. A* **1998**, *102*, 1995–2001.
(28) Cossi, M.; Rega, N.; Scalmani, G.; Barone, V. *J. Comput. Chem.* **2003**, *24*, 669–681.
(29) Cramer, C. J.; Truhlar, D. G. *Chem. Rev.* **1999**, *99*, 2161–2200.
(30) Tomasi, J.; Mennucci, B.; Cammi, R. *Chem. Rev.* **2005**, *105*, 2999–3093.
(31) Marenich, A. V.; Cramer, C. J.; Truhlar, D. G. *J. Phys. Chem. B* **2009**, *113*, 6378–6396.
(32) Benson, S. W. *The Foundations of Chemical Kinetics. s.l.*; Krieger: FL, 1982.
(33) Galano, A. *J. Phys Chem A* **2007**, *111*, 1677–1682.
(34) Alvarez-Idaboy, J. R.; Reyes, L.; Mora-Diez, N. *Org. Biomol Chem.* **2007**, *22*, 3682–3689.
(35) Eyring, H. *J. Chem. Phys.* **1935**, *3*, 107–116.
(36) Evans, M. G.; Polanyi, M. *Trans. Faraday Soc.* **1935**, *31*, 875–894.
(37) Truhlar, D. G.; Hase, W. L.; Hynes, J. T. *J. Phys. Chem.* **1983**, *87*, 2664–2682.
(38) Eckart, C. *Phys. Rev.* **1930**, *35*, 1303–1309.